

DEUTSCHES ELEKTRONEN-SYNCHROTRON
Ein Forschungszentrum der Helmholtz-Gemeinschaft



DESY 21-095
June 2021

**Comment on “Evidence for Parity Violation in
Gravitational Fields” (DESY 18-171)**

T. Behnke, J. List, S. Schmitt, B. Sobloher
Deutsches Elektronen-Synchrotron DESY, Hamburg

ISSN 0418-9833

NOTKESTRASSE 85 – 22607 HAMBURG

DESY behält sich alle Rechte für den Fall der Schutzrechtserteilung und für die wirtschaftliche Verwertung der in diesem Bericht enthaltenen Informationen vor.

DESY reserves all rights for commercial use of information included in this report, especially in case of filing application for or grant of patents.

To be sure that your reports and preprints are promptly included in the
HEP literature database
send them to (if possible by air mail):

DESY Zentralbibliothek Notkestraße 85 22607 Hamburg Germany	DESY Bibliothek Platanenallee 6 15738 Zeuthen Germany
---	---

Comment on “Evidence for parity violation in gravitational fields” (DESY 18-171)

Ties Behnke¹, Jenny List¹, Stefan Schmitt^{1,a} and Blanka Sobloher¹

¹ Deutsches Elektronen-Synchrotron DESY, Notkestr. 85, 22607 Hamburg, Germany

^a corresponding author: sschmitt@mail.desy.de

Abstract

A recent publication (DESY 18-171) claimed evidence for parity violating effects, following an analysis of helicity-dependent energy spectra recorded with the HERA transverse polarimeter. This note is trying to highlight two of the weak points of the analysis. Firstly, the claim of DESY 18-171 is made without presenting a calculation of the Compton cross section in presence of the stated parity violating effects. Secondly, the fit parametrisation given in DESY 18-171 is ill-defined, such that the fit is underconstrained. It is thus concluded that the analysis can not be trusted and the conclusions drawn on “Evidence for parity violation” are invalid.

1 Introduction

In a recent DESY pre-print [1], the claim is made that there is “Evidence for parity violation in gravitational fields”. The apparent observation is made following an analysis of the HERA transverse polarimeter data.

Following the arguments in V. Gharibyan *et al.* [1], the maximum energy of scattered Compton photons is measured, for incident laser photons in two different helicity states. An apparent asymmetry of the two energies is reported and is taken by the authors as evidence for parity violation.

In this paper, comments are made on two aspects of the analysis. In Section 2, a summary of the HERA transverse polarimeter setup and of the energy asymmetry analysis presented in [1] is given. In Section 3, a comment is made on the Compton cross section definition. In Section 4, major deficiencies of the fit functions used in [1] are discussed. A conclusion is drawn at the end.

2 Analysis of the HERA transverse polarimeter data

2.1 Transverse polarimeter setup

The HERA transverse polarimeter [2] was designed to measure the polarisation in the HERA ring. The lepton ring of the HERA collider was operated with electrons or positrons at an energy of up to 27.6 GeV. While the leptons were injected unpolarized at an energy of 12 GeV, they would acquire transverse polarisation at their full energy by means of the Sokolov-Ternov effect [3].

Briefly, the polarimeter setup was as follows: a circularly-polarised laser beam of energy 2.41 eV was brought to collision with the 27.6 GeV lepton beam at a crossing angle of about 3.1 mrad. The laser beam helicity was flipped at a rate of about 80 Hz, using a Pockel’s cell. The back-scattered Compton photons of energies near 14 GeV were detected in a small calorimeter as a distance of about 65 metres from the interaction point, after having separated the lepton and photon beams using two dipole magnets.

The sampling calorimeter was split into two optically isolated halves, such that the vertical impact position of scattered photons would correlate with the energy sharing in the two calorimeter halves. The calorimeter was read out using four photo-multipliers. Wavelength shifters located on the upper (U) and lower side (D) of the calorimeter would only receive light from one of the calorimeter halves. For calibration purposes, there were additional wavelength shifters located on the left (L) and right (R) side. These extended over both calorimeter halves, such that the left and right channels each would receive a sum of scintillating light produced in both halves.

As compared to the original setup, the data acquisition electronics was modernized during the upgrade of the HERA ring for high luminosity between the years 2000–2002. In its upgraded form, the calorimeter channels were read out as follows: following a

pulse shaper, long cables, and an analog noise subtraction, each of the four channels was digitized in a 12-bit sampling ADC operating at 4 times the speed of the HERA bunch clock. An analog sum of the L and R channels was discriminated to provide a trigger signal for calorimeter energies above a threshold near 3.5 GeV. For each trigger, four samples were recorded per channel. In each of the 4 calorimeter channels, a pedestal-subtracted ADC energy was calculated from the four ADC samples $a_{i,c}$ as $E_c = a_{1,c} + a_{2,c} + a_{3,c} - 3a_{4,c}$, where c indicates the respective calorimeter channel (U,D,L,R). Two energy sums were calculated: $E_{LR} = E_L + E_R$ and $E_{UD} = E_U + E_D$. Similarly, two energy asymmetries were calculated as $\eta_{LR} = (E_L - E_R)/E_{LR}$ and $\eta_{UD} = (E_U - E_D)/E_{UD}$. For calibration purposes, also the energy ratio $R = E_{UD}/E_{LR}$ was computed.

The calorimeter data, consisting of the five quantities E_{LR} , E_{UD} , η_{LR} , η_{UD} , and R were not recorded event by event. Instead, the data were directly filled into histograms. Each histogram existed in two versions, depending on the helicity state, or equivalently the Pockel's cell voltage polarity¹. The following histogram types were recorded

- Energy E_{LR} in 8192 bins
- Energy E_{UD} in 8192 bins
- Left-right asymmetry η_{LR} in 128 bins
- Profile plot of the energy ratio R in 128 bins of η_{UD}
- Two-dimensional plot of E_{UD} (64 bins) against η_{UD} (128 bins)

Histograms were accumulated over cycles consisting of laser-off and laser-on data, defined by a chopper wheel, which would block the laser beam when collecting laser-off data. The cycles duration was 45 seconds nominally for the laser-on state and 15 seconds nominally for the laser-off state, minus the time used to rotate the chopper wheel and prepare the data acquisition. The laser-off data serves to estimate background, mainly from Bremsstrahlung emitted by the electron beam off the restgas in the HERA beam line. Typical event rates were 50 kHz for laser-on data and 15 kHz for laser-off data.

The calorimeter was calibrated by iteratively adjusting the photomultiplier high voltage, following an online analysis of the data recorded in one laser-on, laser-off cycle. Similarly, the calorimeter was centred on the beam, by iteratively adjusting the calorimeter table vertical position following the online data analysis of a laser-on, laser-off cycle. The high voltage calibration was necessary on the time scale of weeks, in order to compensate for a slow degradation of the calorimeter due to radiation damage and keep the energy response within an accuracy of 1%. The calorimeter position tracking happened automatically during a HERA fill, in order to track beam movements and keep the beam centred on the calorimeter within $50 \mu\text{m}$. This table centering step typically happened about once per hour, where a HERA fill would last for approximately ten hours.

¹The data were further subdivided into “colliding” and “non-colliding” bunches. The “colliding” bunches, matched by a partner bunch in the HERA proton beam, typically had larger emittances and smaller polarisation as compared to the “non-colliding” bunches. For the present analysis, data of these two bunch groups are added up.

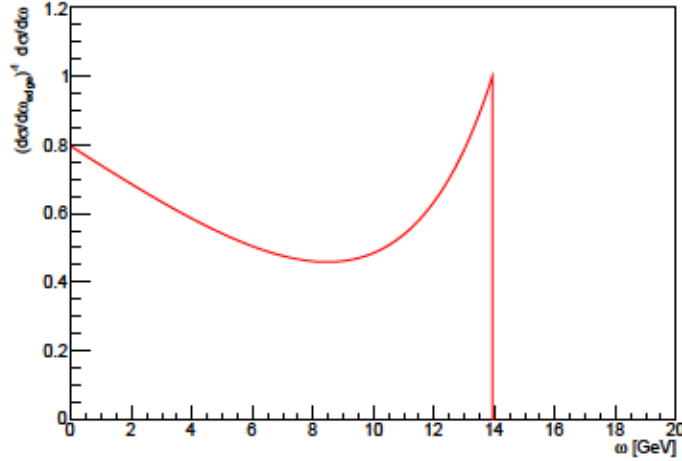


Figure 1: Unpolarized cross section as a function of photon energy ω for Compton backscattering of laser photons with energy 2.41 eV off an electron beam of 27.6 GeV. The differential cross section is normalized to unity at the maximum photon energy ω_{edge}

2.2 Compton cross section and calorimeter calibration

The unpolarized Compton cross section as a function of the backscattered photon energy ω^{SM} , expressed as a function of the energy fraction relative to the lepton beam energy $x = \omega^{\text{SM}}/E_{\text{beam}}$, is given by [2]

$$\frac{d\sigma^{\text{SM}}}{d\omega^{\text{SM}}} = \begin{cases} K \frac{2-2x(2+2/k_i)+x^2(2+(1+1/k_i)^2)-x^3}{(1-x)^2} & \text{for } x \leq x_{\text{edge}} \\ 0 & \text{for } x > x_{\text{edge}} \end{cases} \quad (1)$$

where $k_i = 2E_{\text{beam}}E_\lambda/m_e^2$ depends on the lepton beam energy, the incoming laser photon energy E_λ and the electron mass m_e ; $x_{\text{edge}} = 2/(2+1/k_i)$ is the maximum energy fraction taken by the backscattered photon relative to the beam energy; K is a normalisation constant. The maximum photon energy $\omega_{\text{edge}} = E_{\text{beam}}x_{\text{edge}}$ is often referred to as ‘‘Compton edge’’. The indices SM on the cross section definition indicate that this corresponds to the ‘‘standard model’’ definition of Compton scattering. At HERA $E_{\text{beam}} = 27.6$ GeV and the laser energy was chosen as $E_\lambda = 2.41$ eV, such that $k_i = 0.509$, $x_{\text{edge}} = 0.505$ and the Compton edge was at $\omega_{\text{edge}} = 13.9$ GeV. The resulting cross section, normalized to the cross section at the Compton edge, is shown in figure 1.

For a polarized lepton beam or a polarized laser, the cross section formula receives additional terms, also depending on the azimuthal scattering angle. While these terms were explored for the primary purpose of the polarimeter, for measuring the lepton beam polarisation [2], they vanish at the Compton edge and are not relevant for the discussion in this note.

The high energy Compton photons were scattered into a small cone. At the calorimeter surface there was an additional broadening of the impact position distribution, related

to the Twiss parameters of the lepton beam and the properties of the laser beam. At HERA, the typical size of the Compton beam at the calorimeter was about 0.5 mm in the vertical and a few mm in the horizontal.

2.3 The DESY 18-171 Analysis of energy spectra and their asymmetries

The analysis [1] of energy spectra is summarized in this paragraph. It is based on the histograms of the quantity $E = E_{LR}$. Laser-off cycles are paired with laser-on cycles. The laser-off data are re-normalized and subtracted from the laser-on data. The two laser-helicity states are kept in separate histograms. These background-subtracted data are fitted in a narrow energy range around the nominal Compton edge position. A simultaneous fit with six free parameters is employed to the two histograms corresponding to the two helicity states. The energy ranges correspond to approximately $12.6 < E < 15.8$ GeV, where the calorimeter energy resolution at 14 GeV is about 0.9 GeV. The two fit functions (for the two helicity states) share parameters C for the overall energy calibration and σ_0 for the overall calorimeter resolution, while there are helicity-dependent parameters for normalisation N_λ and Compton edge position ω_λ (the two helicity states labelled $\lambda = \pm 1$). The fit functions are defined as [1]

$$F_\lambda(E) = N_\lambda \int_0^{\omega_\lambda} \frac{d\Sigma}{d\omega} \frac{1}{\sqrt{\omega}} \exp \left[\frac{-(\omega - CE)^2}{2\sigma_0^2\omega} \right] d\omega, \quad (2)$$

without specifying in detail how the Compton cross section $\frac{d\Sigma}{d\omega}$ is evaluated. For claiming effects beyond the standard model, in [1] finally the Compton edge asymmetry $A = (\omega_{+1} - \omega_{-1})/(\omega_{+1} + \omega_{-1})$ is averaged over many cycles and is found to be non-zero. The non-zero average A is interpreted as an ‘‘Evidence of parity violation in gravitational fields’’.

3 Comment on the Compton Cross section definition

The ‘‘theoretical’’ basis of the analysis [1] is a simple calculation of the maximum photon energy, after modifying the photon’s dispersion relation by introducing a refraction index different from unity. Energy-momentum conservation is invoked in the laboratory frame, and the maximum possible photon energy is calculated. That kinematic effect is such that the expected maximum energy ω_λ of a scattered Compton photon is different from the ‘‘standard model’’ value ω_{edge} . The magnitude of the effect is found to be proportional to the difference of the refraction index from unity, enhanced by the square of the electron’s Lorentz boost factor, i.e. the ratio of incoming electron beam energy to electron rest mass.

One problem with this *ansatz* is that this ‘‘theory’’ is incomplete. Only the change in the maximum energy is calculated, but it is not determined how that would reflect consistently in a change of the cross section shape. So, even if the apparent asymmetry was a firm experimental result, its interpretation will have to remain unclear.

For having a deeper look at the fit function in the next section, it would have been interesting to know the cross section definition used for the fits in [1]. In the following, two possible *ad hoc* cross section definitions are described.

Energy scaling the assumption is made that the shape of the Compton cross section remains unchanged, so the scattered photon energy is rescaled by the ratio $\omega_\lambda/\omega_{\text{edge}}$,

$$\frac{d\sigma^{\text{scaled}}}{d\omega^{\text{scaled}}} = \frac{d\sigma^{\text{SM}}}{d\omega^{\text{SM}}} \Big|_{\omega^{\text{SM}} = \omega^{\text{scaled}} \frac{\omega_{\text{edge}}}{\omega_\lambda}}. \quad (3)$$

Compton edge shift the assumption is made that only the Compton edge shifts, so in the Compton cross section formula 1 only the quantity x_{edge} is scaled by the ratio $\omega_\lambda/\omega_{\text{edge}}$. In other words, the cross section for a given photon energy is numerically identical to the “standard model” however the range in x where the cross section is valid is changed,

$$\frac{d\sigma^{\text{shift}}}{d\omega^{\text{shift}}} = \frac{d\sigma^{\text{SM}}}{d\omega^{\text{SM}}} \Big|_{\omega^{\text{SM}} = \omega^{\text{shift}} \text{ and } x_{\text{edge}} \rightarrow x_{\text{edge}} \frac{\omega_\lambda}{\omega_{\text{edge}}}}. \quad (4)$$

4 Comment on the improper choice of parametrisation

The background-subtracted data are fitted in [1] by a six-parameter function, equation 2. As will be shown here, that fit function has an underconstrained parameter set for the chosen data, so the fit results are ill-defined.

Qualitatively, the deficit in the parametrisation can be understood as follows: the function equation 2 is very similar to a simple threshold function,

$$F_\lambda(E) \sim K \times \text{erfc} \left[\frac{E - \omega_\lambda/C}{\sqrt{2\omega_\lambda\sigma_0/C}} \right]. \quad (5)$$

Also compare to figure 3 of [1], lower subfigure. Such a threshold function only can constrain three parameters: the *normalisation* K , the *threshold* ω_λ/C , and the *width* $\sqrt{\omega_\lambda\sigma_0}/C$. Leaving aside the *normalisation* parameter, there is no possibility to determine the three quantities C , ω_λ and σ_0 simultaneously, given the knowledge of only two parameters, *threshold* and *width*.

When using two spectra instead of one, the situation is a bit more complex. Indeed it would have been possible to determine six parameters (two normalisation constants, two threshold parameters and two widths). However, the particular set of six parameters chosen in equation 2 is not permitted, as will be shown below.

The fit parameter degeneracy is most obvious for the case of the cross section with “Energy scaling” by substituting $\omega = \omega^{\text{SM}} \frac{\omega_\lambda}{\omega_{\text{edge}}}$

$$F_\lambda^{\text{scaled}}(E) = N_\lambda \int_0^{\omega_\lambda} \frac{d\sigma^{\text{SM}}}{d\omega^{\text{SM}}} \Big|_{\omega^{\text{SM}} = \omega \frac{\omega_{\text{edge}}}{\omega_\lambda}} \frac{1}{\sqrt{\omega}} \exp \left[\frac{-(\omega - CE)^2}{2\sigma_0^2 \omega} \right] d\omega \quad (6)$$

$$= N_\lambda \sqrt{\frac{\omega_\lambda}{\omega_{\text{edge}}}} \int_0^{\omega_{\text{edge}}} \frac{d\sigma^{\text{SM}}}{d\omega^{\text{SM}}} \frac{1}{\sqrt{\omega^{\text{SM}}}} \exp \left[\frac{-(\omega^{\text{SM}} \frac{\omega_\lambda}{\omega_{\text{edge}}} - CE)^2}{2\sigma_0^2 \omega^{\text{SM}} \frac{\omega_\lambda}{\omega_{\text{edge}}}} \right] d\omega^{\text{SM}} \quad (7)$$

In this form it is evident that the fit parameters can be scaled by an arbitrary constant $k > 0$ as follows

$$C \rightarrow k \times C \quad (8)$$

$$\omega_\lambda \rightarrow k \times \omega_\lambda \quad (9)$$

$$\sigma_0 \rightarrow \sqrt{k} \times \sigma_0 \quad (10)$$

$$N_\lambda \rightarrow \frac{1}{\sqrt{k}} \times N_\lambda \quad (11)$$

without changing the fit function. In other words, of the *six* parameters C , ω_{-1} , ω_{+1} , σ_0 , N_{-1} , N_{+1} only *five* are independent. The “Energy scaling” cross section definition is not compatible with a fit to the chosen parameter set.

For the case of the cross section with the “shifted Compton edge” or any other cross section form, a simplified fit function is considered here to make the argument. For the simplified function, the Compton cross section is replaced by a constant, which is taken to be unity. This simplification is justified, because in [1] the data intentionally are probed only in a narrow range around the Compton edge. The two simplified fit functions (for $\lambda = \pm 1$) thus look like this:

$$F_\lambda^{\text{simplified}}(E) = N_\lambda \int_0^{\omega_\lambda} \frac{1}{\sqrt{\omega}} \exp \left[\frac{-(\omega - CE)^2}{2\sigma_0^2 \omega} \right] d\omega \quad (12)$$

$$= N_\lambda \sigma_0 \sqrt{\frac{\pi}{2}} \left(\text{erfc} \left[\frac{CE - \omega_\lambda}{\sqrt{2\omega_\lambda} \sigma_0} \right] - \exp \left[2 \frac{CE}{\sigma_0^2} \right] \text{erfc} \left[\frac{CE + \omega_\lambda}{\sqrt{2\omega_\lambda} \sigma_0} \right] \right) \quad (13)$$

For the simplified fit function, again the fit parameters are not independent of each other and can be scaled by an arbitrary constant $k > 0$ as shown in equations 8-11 without affecting the predicted ADC spectra.

Ultimately, when using the proper cross section definition, the fit parameter degeneracy visible in equation 13 possibly could be resolved, at the cost of including data from a larger energy range. The range will have to be chosen such that the constant C can be constrained independently of the parameters ω_λ . For example, the exotic theory could possibly predict that the minimum of the Compton cross section (near 8 GeV in figure 1) will remain invariant under the change of ω_λ , and that would indeed help to constrain the parameter C .

However, given the narrow fit range of the present analysis, correlation coefficients of the fit parameters will be very close to unity, even if a cross section definition was

used which is able to decorrelate the parameters to some extent. The fits are done using the gradient-based minimizer MINUIT [4]. Gradient based algorithms have difficulties to deal with highly correlated parameter sets. Such fits typically exhibit large sensitivity to numerical effects (as for example caused by numerical integration) and also to the choice of starting parameters. In other words, the results of the fits can not be trusted and hence the subsequent analysis of the resulting apparent asymmetries is meaningless.

5 Conclusions

Two comments are made with respect to a recent paper claiming “Evidence for Parity Violation in Gravitational Fields”. It is shown that the claim made in that paper is based on an incomplete formulation of the cross sections it is trying to probe. Even worse, the parameter set chosen with the fit function is not constrained sufficiently well by the data which are used. As such, the fit results can not be considered to be reliable. In summary, the data analysis presented in that paper does not define what precisely is measured and uses improper analysis methods, so the conclusions drawn therein on “Evidence for Parity Violation in Gravitational Fields” are not valid.

References

- [1] V. Gharibyan *et al.*, “Evidence for Parity Violation in Gravitational Fields”, DESY 18-171
- [2] D. P. Barber *et al.*, Nucl. Instrum. Meth. A **329** (1993) 79.
doi:10.1016/0168-9002(93)90924-7
- [3] A. A. Sokolov and I. M. Ternov, Dokl. Akad. Nauk SSSR **153** (1963) no.5,
1052-1054
- [4] F. James and M. Roos, Comput. Phys. Commun. **10** (1975), 343-367
doi:10.1016/0010-4655(75)90039-9